

## Facile and Eco-friendly One Step Low Temperature Synthesis of Very Large Scale $\text{ATiO}_3$ (A = Ca, Sr, Ba and Cd)

Pramendra Kumar Pandey<sup>1</sup>, Revati Raman Chaubey<sup>2</sup>, Gyandeshwar K Rao<sup>3</sup>, Suman Srivastava<sup>1</sup>, Arvind Kumar Singh<sup>4</sup> and Bharat Kumar<sup>1\*</sup>

<sup>1</sup>Department of Chemistry, M V College Buxar (Constituent unit of Veer Kunwar Singh University Ara), India

<sup>2</sup>Department of Chemistry, Indira Gandhi National Tribal University Amarkantak, India

<sup>3</sup>Department of Chemistry, Kisan College Nalanda (Constituent unit of Patliputra University Patna), India

<sup>4</sup>Department of Chemistry, S B College Ara (Constituent unit of Veer Kunwar Singh University Ara), India

### \*Corresponding Author

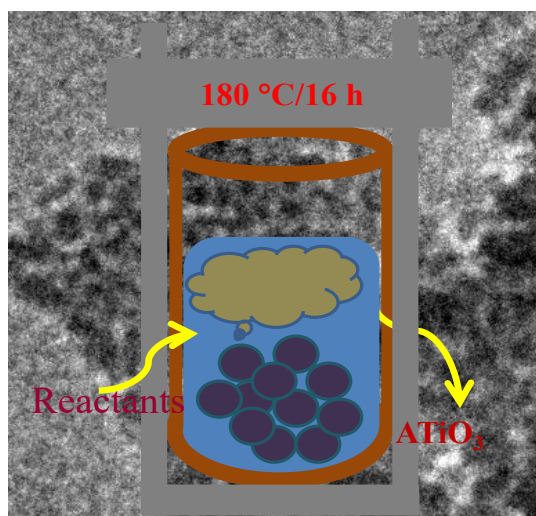
Bharat Kumar, Department of Chemistry, M V College Buxar (Constituent unit of Veer Kunwar Singh University Ara), India.

Submitted: 2025, Dec 30; Accepted: 2026, Jan 26; Published: 2026, Feb 04

**Citation:** Pandey, P. K., Chaubey, R. R., Rao, G. K., Srivastava, S., Kumar, B., et al. (2026). Facile and Eco-friendly One Step Low Temperature Synthesis of Very Large Scale  $\text{ATiO}_3$  (A = Ca, Sr, Ba and Cd). *J App Mat Sci & Engg Res*, 10(1), 01-10.

### Abstract

The primary motivation of this work is to develop a low-cost and scalable methodology for the synthesis of industrially significant metal titanates. In this study,  $\text{ATiO}_3$  (A = Ca, Sr, Ba, and Cd) perovskite nanoparticles were successfully synthesized via a simple, one-step hydrothermal process carried out at 180 °C for 16 hours. By varying the titanium precursor from  $\text{TiO}_2$  to titanium isopropoxide, nanoparticles with different sizes and morphologies were obtained. This approach offers a general and practical route for the large-scale synthesis of  $\text{ATiO}_3$  perovskite materials.



## Highlights

- Low temperature general synthesis protocol for 4 titanates
- Variation of reactant phase from solid to liquid and their effect of morphology
- Hollow rectangle shape morphology of  $\text{CaTiO}_3$
- Enhancement in the surface area of  $\text{BaTiO}_3$
- Scope of applications in various industry

**Keywords:** Hydrothermal, Titanium Isopropoxide, Titanates, Hollow

## 1. Introduction

Nanostructured materials such as nanoparticles, nano cubes, nanorods, nanotubes and nanowires are under intensive investigation due to their size and shape dependent properties and potential application in the all field of technology due to their thermal, electrical, mechanical and optical properties [1-5]. Among the nanostructured materials, perovskite with general formulae  $\text{ABO}_3$  constitute important classes of materials in solid state chemistry due their wide applicability in ferroelectrics, dielectric, piezoelectric nonlinear optics properties with their technology importance for fabricating the different class of devices [6-10]. On the commercial scale, these oxide powders are produced at high-temperature which's chemical in homogeneity, reactivity problems and very little control on the size, shape and agglomeration. Due to these above problems, there is demand for the low temperature synthesis route to yield high-purity fine powders with controlled size and morphology for miniaturization of these materials to the nanometer scale for the next generation of electronics.

All the titanates are useful class of materials due to their industrial application in various technologies. Among them  $\text{BaTiO}_3$ ,  $\text{SrTiO}_3$ , and  $\text{CaTiO}_3$  has more importance.  $\text{BaTiO}_3$  has ferroelectric property, high dielectric constant and positive temperature coefficient of resistivity (PTCR) used as multilayered ceramic capacitors (MLCCs), embedded decoupling capacitors (EDC), thermistor, waveguide modulators, IR detectors, microwave absorbers, dynamic random access memory and field - effect transistors [11-15].  $\text{SrTiO}_3$  is an important n-type semiconductor with band gap between 3.2 – 3.4 eV have high dielectric constant, thermal and chemical stability. It has a wide application in field of thin-film capacitors, nonlinear optics, optical memories, oxygen gas sensors, photocatalyst and photoelectrode for splitting of water, solar cell and electrooptic modulators [16-19].  $\text{CaTiO}_3$  crystallizes in orthorhombic crystal system with space group (Pbnm). It has various applications such as component of capacitors, immobilization of nuclear wastes, mineralogy, microwave dielectric applications (as resonators and filters), luminescent material and biomedical area [20-23].  $\text{CdTiO}_3$  crystallizes in non-

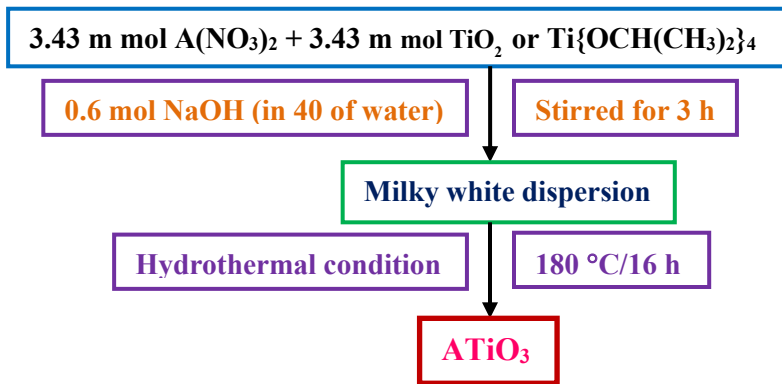
ferroelectric ilmenite rhombohedral crystal system. Below the 1000 °C annealing temperature is an intelligent material due to their application in optical fiber and sensor [24, 25]. It has also piezoelectric, pyroelectric, magneto restrictive and photostrictive properties [26-28].

There are various reports for synthesizing such titanates by solid state, sol – gel, hydrothermal, microwave hydrothermal method, spray pyrolysis, microemulsion, polymeric precursor and coprecipitation [29-37]. There are few reports for general methodology of the  $\text{MTiO}_3$  nanoparticles [38-41]. There are reports of the synthesis of  $\text{SrTiO}_3$  and  $\text{BaTiO}_3$  at low temperature however there is no any such report on  $\text{CaTiO}_3$  and  $\text{CdTiO}_3$  at low temperature [42-46]. There is no general approach reported for synthesizing the above four compounds by a single step on large scale.

In this letter, we report the synthesis of  $\text{ATiO}_3$  (A = Ca, Sr, Ba, and Cd) perovskite materials using two different titanium sources: titanium dioxide and titanium isopropoxide. The resulting compounds were thoroughly characterized using powder X-ray diffraction (PXRD), field emission scanning electron microscopy (FESEM), transmission electron microscopy (TEM), Brunauer–Emmett–Teller (BET) surface area analysis, and UV-Visible diffuse reflectance spectroscopy (DRS).

## 2. Synthesis and Characterization

$\text{ATiO}_3$  nanoparticles were synthesized by hydrothermal route. In typical synthesis process 3.43 m mol of  $\text{A}(\text{NO}_3)_2$  was dissolve in 20 ml of double distilled water followed addition of 3.43 m mol of  $\text{TiO}_2$  (Titanium isopropoxide also). The above solution was stirred for 30 min and then 0.6 mol NaOH dissolved in 40 ml of water were added and stirred for 3 h. The obtained milky white solution was transferred to teflon beaker and putted inside the stainless-steel hydrothermal bomb and placed in oven at 180°C for 16 h. The schematic diagram for the synthesis of  $\text{ATiO}_3$  nanoparticles of different morphology is given in scheme 1.

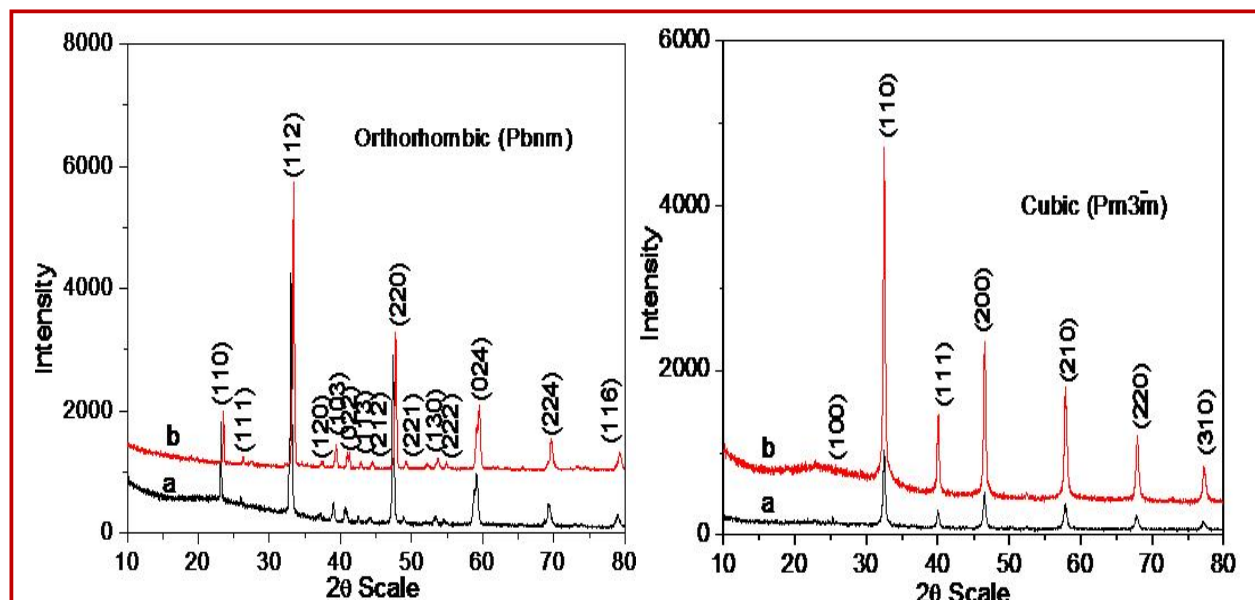


**Scheme 1: General Procedure for the Synthesis of  $\text{ATiO}_3$**

Powder X-ray diffraction studies (PXRD) were carried out using Ni filtered  $\text{Cu-K}\alpha$  radiation. Normal scans were recorded with a step size of  $0.02^\circ$  and step time of 1 s. The  $\text{K}\alpha_2$  reflections were removed to obtain accurate lattice constants. Field emission scanning electron microscopy (FESEM) was carried out by FEI quanta 3D FEG – FESEM operated at 10 kV. The pellet had been coated with gold. Transmission Electron Microscopy (TEM) studies were carried out using a Tecnai G2 20 electron microscope operated at 200 KV. TEM specimens were prepared by dispersing the sample in ethanol by ultrasonic treatment, dropping onto a porous carbon film supported on a copper grid, and then drying in air. Nitrogen adsorption–desorption isotherms were recorded at liquid nitrogen temperature (77 K) using a Nova 2000e (Quantachrome Corp.) equipment and the specific area was determined by the Brunauer–Emmett–Teller (BET) method. The powder sample was degassed at  $150^\circ\text{C}$  for 6 h prior to the surface area measurements. Diffuse-reflectance spectra (DR) spectra were recorded on Shimadzu UV-2450 spectrophotometer where the baseline was fixed using a barium sulfate reference.

### 3. Result and Discussion

The aim behind this study is to develop a low-cost methodology for the synthesis of important titanates with different morphology at very low temperature. Here we have developed a common one step synthesis protocol at very low temperature ( $180^\circ\text{C}$ ) to synthesize titanates at gram scale ( $\sim 1\text{g}$ ) level by hydrothermal route. Here we fixed the hydrothermal reaction time, temperatures, reactant and base concentration. We varied the one of the reactant (Ti source) phase from solid to liquid to see change in the morphology. Using a NaOH base, we obtained pure phase of the nanocrystalline titanates  $\text{ATiO}_3$  (Ca, Sr, Ba, Cd). Figures 1 (A, B, C, D) show the powder X-ray diffraction patterns of  $\text{CaTiO}_3$ ,  $\text{SrTiO}_3$ ,  $\text{BaTiO}_3$  and  $\text{CdTiO}_3$  respectively using both  $\text{TiO}_2$  and titanium isopropoxide as Ti source. The PXRD patterns confirm the formation of monophasic nature for all the eight titanates. All the observed diffraction patterns were indexed on the basis of their crystal structures. The lattice parameters were refined and it observed that in case of titanium isopropoxide as Ti source the values was lower as compared to  $\text{TiO}_2$  as Ti source due to decrease in the particles size of corresponding titanates.



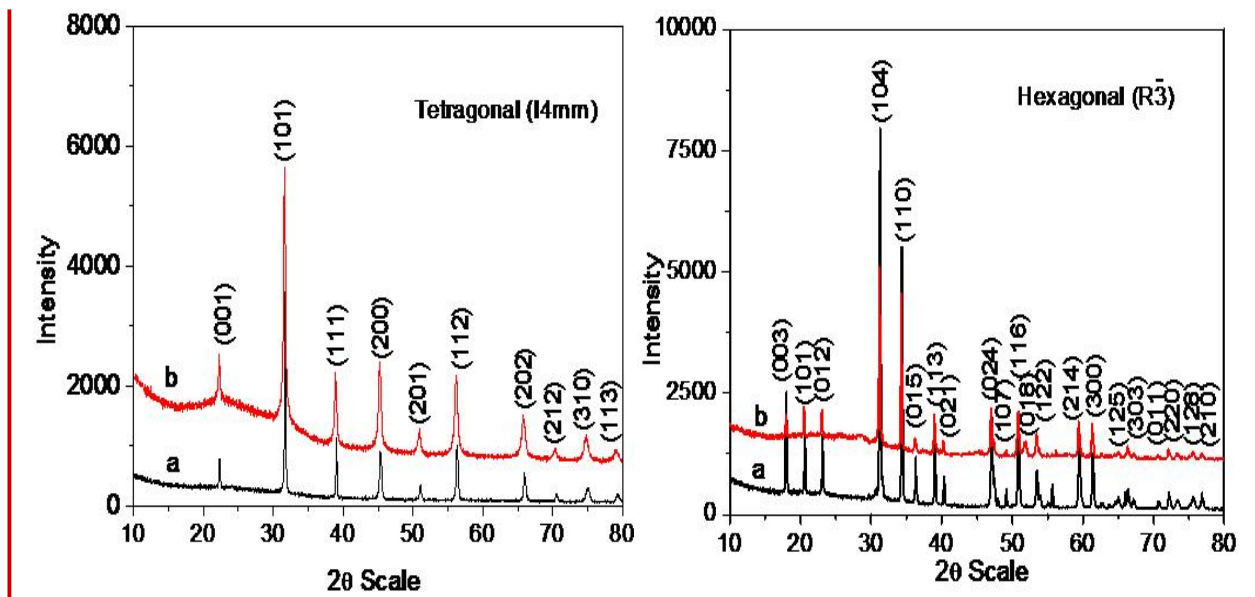
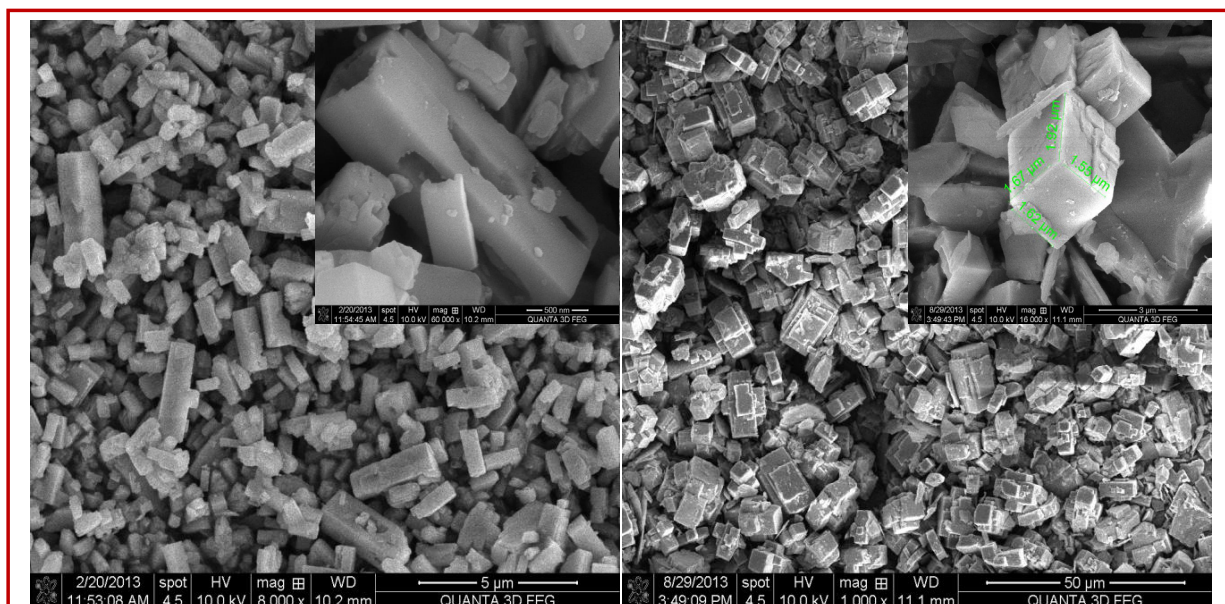
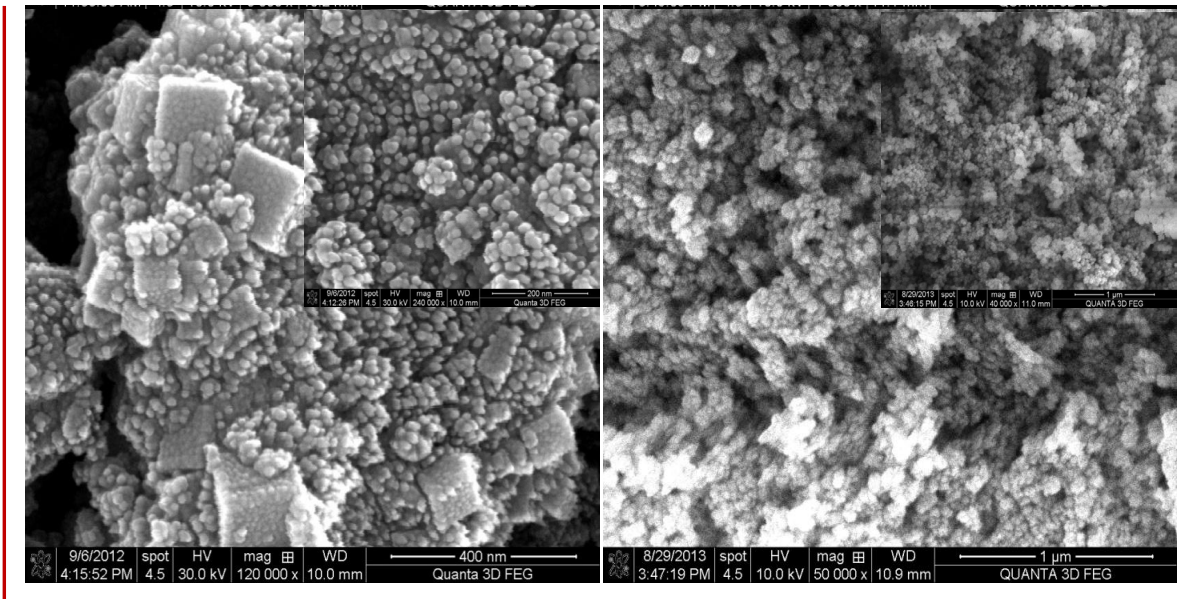


Figure 1: Powder x-ray Diffraction Pattern of (A)  $\text{CaTiO}_3$  (B)  $\text{SrTiO}_3$  (C)  $\text{BaTiO}_3$  (D)  $\text{CdTiO}_3$

Field emission scanning electron microscopy was carried out to check the morphology of these synthesized titanates. Figure 2 and 3 show the field emission scanning electron micrograph of titanates. Figure 2a shows cube shape morphology of  $\text{CaTiO}_3$  obtained using  $\text{TiO}_2$  whereas in case of titanium isopropoxide (Figure 2b), rectangle hollow shape morphology was obtained. This result clearly indicates that with change in source phase from solid ( $\text{TiO}_2$ ) to liquid (titanium isopropoxide) the morphology was changed. This hollow morphology type's materials are very interesting for various applications such as drug delivery and catalysis [47-49]. The  $\text{SrTiO}_3$  (Figure 2c and 2d) the particles are spherical in nature having two different sizes for the two different titanium sources.

For the titanium isopropoxide source, the particles are smaller as compared to titanium dioxide. In the case of  $\text{TiO}_2$  source some of these nanoparticles (30 nm size) are aggregated and form cube shaped structures. The  $\text{BaTiO}_3$  nanoparticles size distribution (Figure 3b) is very uniform in case of titanium isopropoxide as Ti source and it is found to be very small in size (further confirm by TEM) as compared to  $\text{TiO}_2$  sources. The  $\text{BaTiO}_3$  obtained from  $\text{TiO}_2$  (Figure 3a) shows the formation of mixed morphology i.e. spherical and cube. For  $\text{CdTiO}_3$ , sheet like morphology was obtained in both the cases. The size of sheet is smaller and broken in case of liquid phase sources. These sheets like structures are very useful for the formation of 2-D materials for practical applications.





**Figure 2:** FESEM Micrograph of (a, b)  $\text{CaTiO}_3$  (c, d)  $\text{SrTiO}_3$  using  $\text{TiO}_2$  and Titanium Isopropoxide as Ti Source Respectively

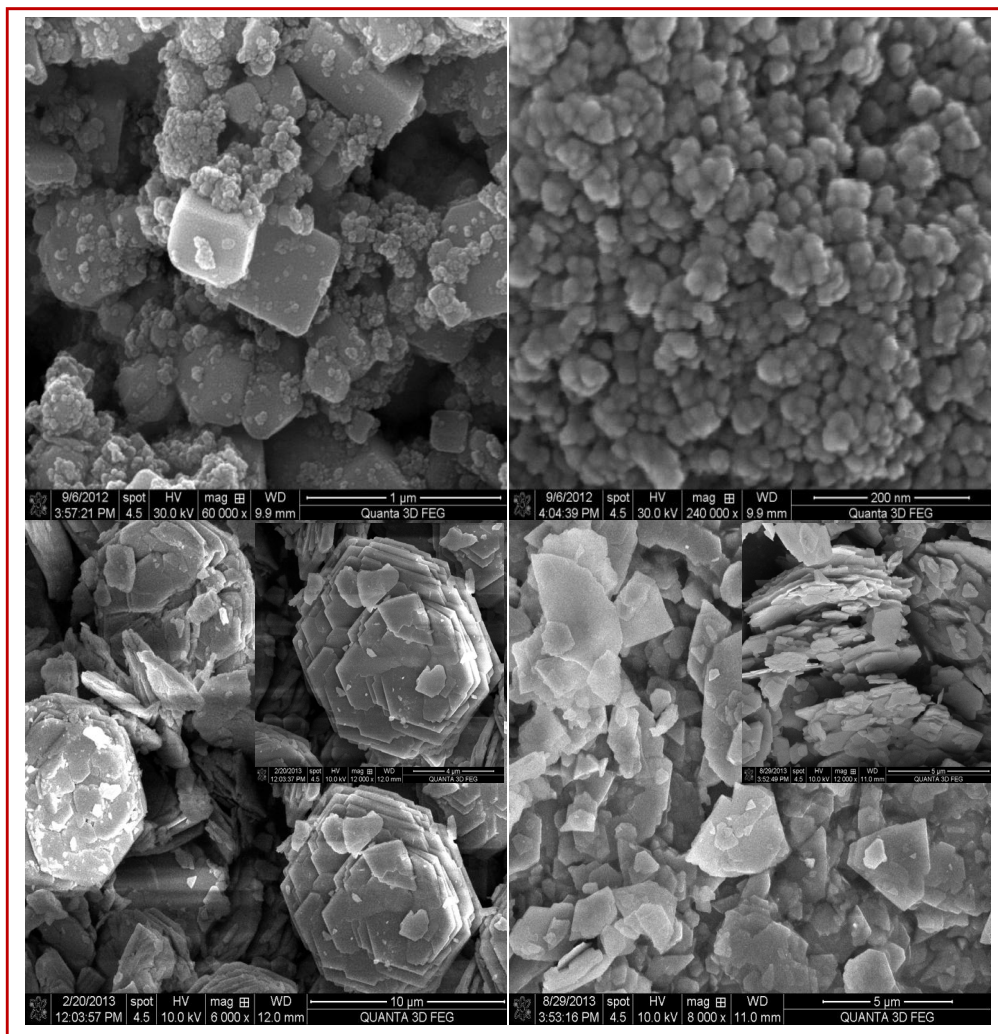


**Figure 3:** FESEM Micrograph of (a, b)  $\text{BaTiO}_3$  (c, d)  $\text{CdTiO}_3$  using  $\text{TiO}_2$  and Titanium Isopropoxide as Ti Source Respectively

Transmission electron microscopy (Figure 4) was carried out to confirm the particle size of  $\text{SrTiO}_3$  and  $\text{BaTiO}_3$  nanoparticles. The  $\text{SrTiO}_3$  nanoparticles (Figure 4a and 4b) are spherical in nature having average particles size of 30 nm and 12 nm for titanium dioxide and titanium isopropoxide respectively. There are very few reports of  $\text{SrTiO}_3$  having particles of size less than 15 nm but none of the reports claim synthesis at gram scale level [50, 51]. The  $\text{BaTiO}_3$  nanoparticles are uniformly distributed and spherical

in nature in case of titanium isopropoxide as titanium sources (Figure 4d). The average diameter of the particles was found to be 5 nm. In case of metal titanates obtained from  $\text{TiO}_2$  source showed mixed distribution of particle size (Figure 4c). There are only some reports in literature of  $\text{BaTiO}_3$  of such small size nanoparticles however the synthesis method not showed a general protocol [42-46, 51].

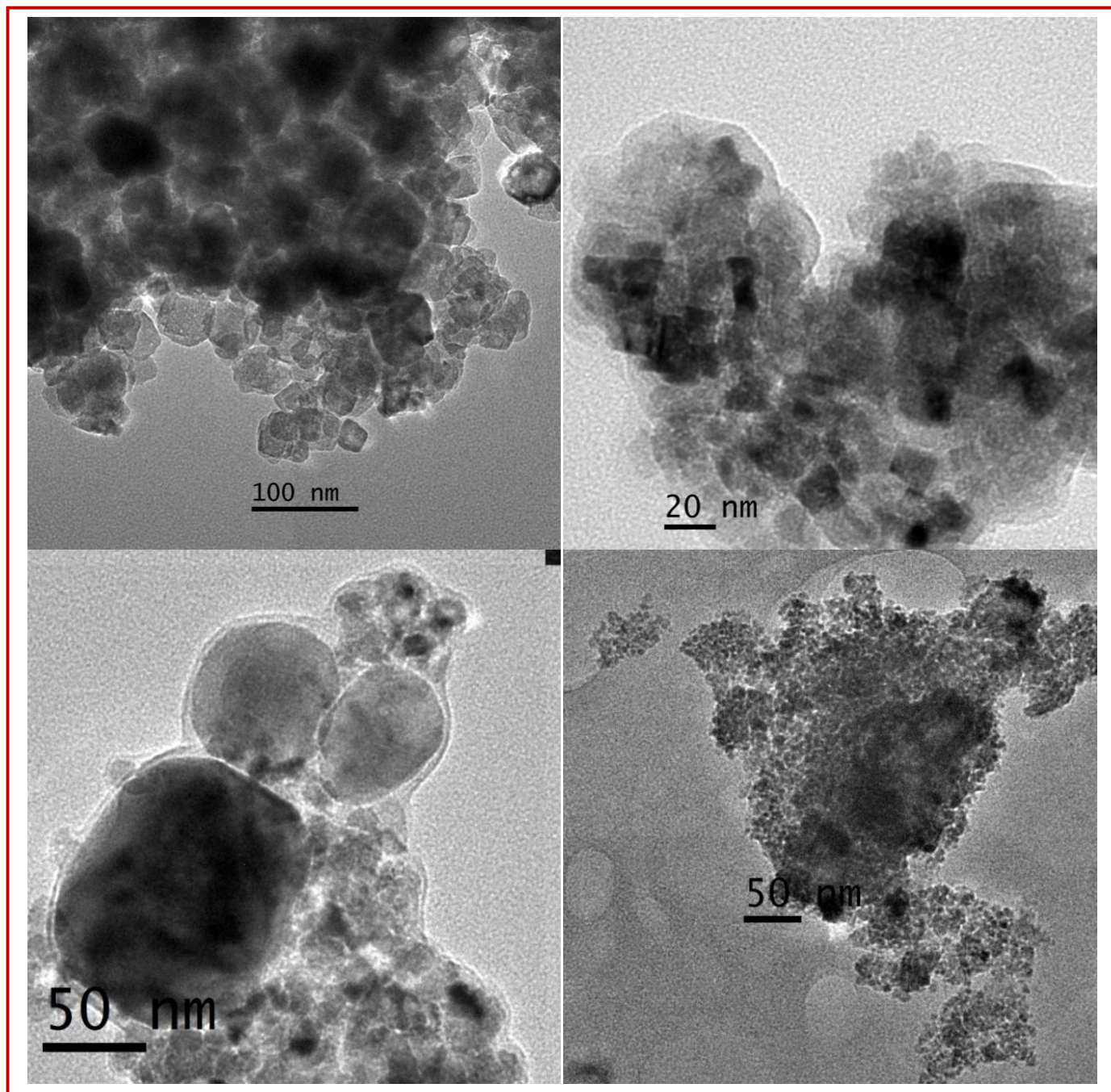


**Figure 4:** TEM Micrograph of (a, b)  $\text{SrTiO}_3$  (c, d)  $\text{BaTiO}_3$  using  $\text{TiO}_2$  and Titanium Isopropoxide as Ti Source Respectively

$N_2$  adsorption-desorption measurement was carried out for surface area measurements of the nanoparticles (Table 1). It was observed that as titanium source changed from solid phase ( $TiO_2$ ) to liquid phase (titanium isopropoxide) the surface area of the titanates enhanced along with decrease in particle size. In case of  $CaTiO_3$  and  $BaTiO_3$ , the surface area is more enhanced due to the hollow shape particles ( $CaTiO_3$ ) and small in  $BaTiO_3$  in case of titanium isopropoxide as Ti sources.

Figure 5 shows the diffuse reflectance spectra of the all the titanates. It was observed that as titanium source changed from  $TiO_2$  to titanium isopropoxide the band gap of the titanates increased due to decrease in particle size. All the titanates have band gap in the UV and close to the reported value. The optical properties (band gap) of nanomaterials are size and morphology dependent [52, 53]. For several cases, it is observed that a change in size and morphology can alter the band gap. The band gap of all the titanates is given in Table 1.

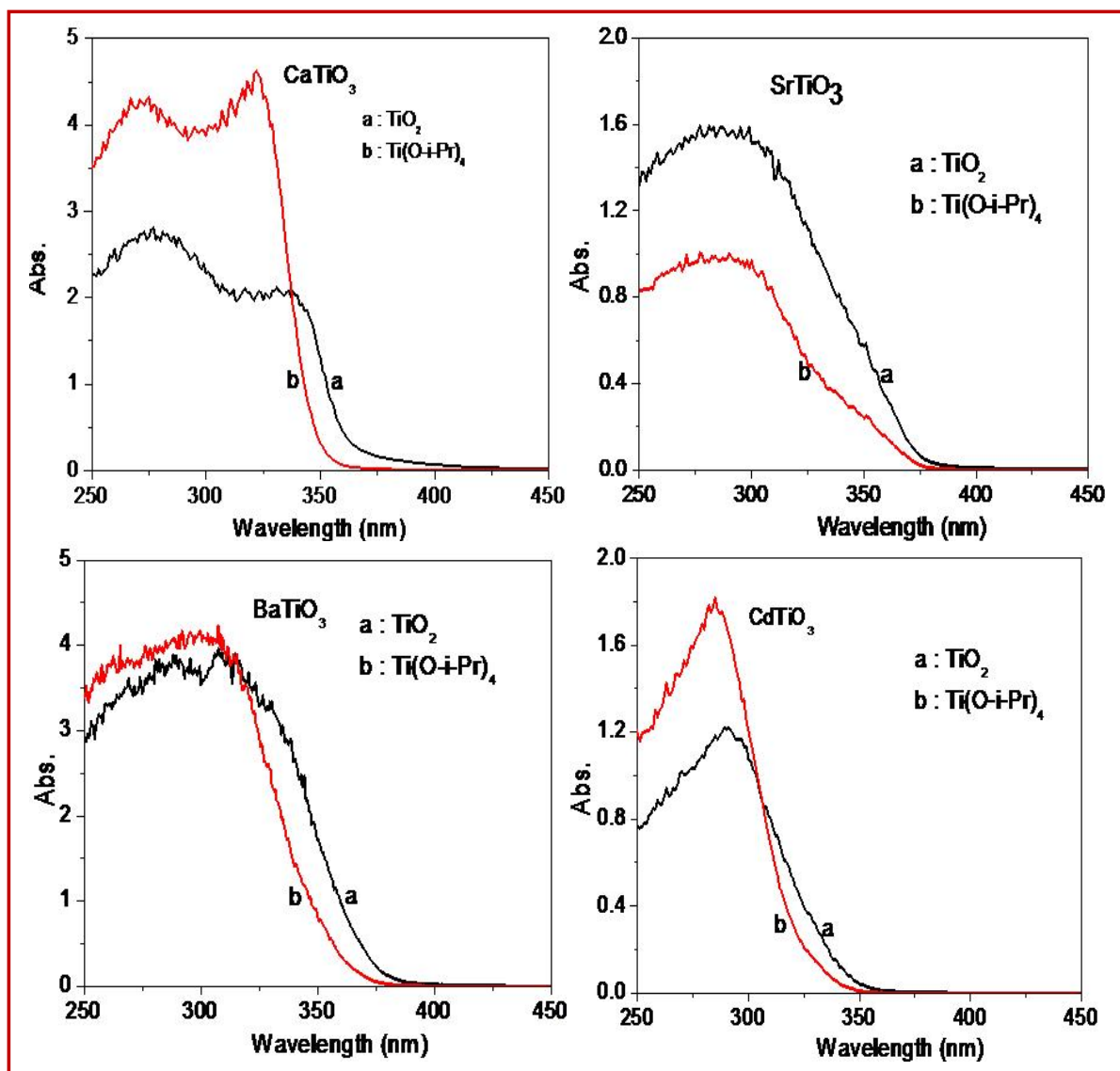


Figure 5: Diffuse Reflectance Spectra of (A)  $CaTiO_3$  (B)  $SrTiO_3$  (C)  $BaTiO_3$  (D)  $CdTiO_3$

S. No.	Compound	Ti Source	Surface area ( $g/m^2$ )	Band Gap (eV)
1	$CaTiO_3$	$TiO_2$	49	3.4
		$Ti(O-i-Pr)_4$	152	3.5
2	$SrTiO_3$	$TiO_2$	55	3.3
		$Ti(O-i-Pr)_4$	64	3.35

3	BaTiO <sub>3</sub>	TiO <sub>2</sub>	58	3.3
		Ti(O-i-Pr) <sub>4</sub>	184	3.4
4	CdTiO <sub>3</sub>	TiO <sub>2</sub>	67	3.6
		Ti(O-i-Pr) <sub>4</sub>	95	3.7

**Table 1: Surface Area and Band Gap of Synthesized Titanates**

#### 4. Conclusions

We report a general and cost-effective one-step hydrothermal protocol for the low-temperature synthesis of CaTiO<sub>3</sub>, SrTiO<sub>3</sub>, BaTiO<sub>3</sub>, and CdTiO<sub>3</sub> nanoparticles. The morphology and particle size are strongly influenced by the titanium precursor, with liquid-phase titanium isopropoxide producing significantly smaller and more uniformly distributed nanoparticles than TiO<sub>2</sub>; in particular, BaTiO<sub>3</sub> nanoparticles as small as ~5 nm were obtained. The size and morphology can be further tuned by varying hydrothermal parameters such as reaction time, temperature, base, and reactant concentration. The successful synthesis of ultra-small titanate nanoparticles at low temperatures and in large quantities demonstrates the scalability of this approach and highlights its potential for commercial production of nanostructured metal titanates.

#### Acknowledgments

PKP and BK thanks ANRF for providing support through the grant no SUR/2022/004717. The authors also thank IIT Delhi India for some of reaction and characterization facility.

#### Author Contributions

Pramendra Kumar Pandey and Revati Raman Chaubey: Synthesis and draft writing, Gyandeshwar Kumar Rao, Suman Srivastava and Arvind Kumar Singh: Characterization, Bharat Kumar: Concept, synthesis modification, final draft writing and final submission. All the authors reviewed the manuscript.

#### Funding

Funding is not applicable

#### Declarations

##### Clinical Trial

Clinical trial is not applicable in the manuscript.

#### Consent to Publish Declaration

Not applicable

#### Ethics and Consent to Participate Declarations:

Not applicable

#### Competing Interests:

The authors declare no competing interests.

#### Data Availability

The authors declare that the data supporting the findings of this study are available within the paper file. Should any raw data files be needed in another format they are available from the

corresponding author upon reasonable request.

#### References

- He, Y. B., Li, G. R., Wang, Z. L., Su, C. Y., & Tong, Y. X. (2011). Single-crystal ZnO nanorod/amorphous and nanoporous metal oxide shell composites: Controllable electrochemical synthesis and enhanced supercapacitor performances. *Energy & Environmental Science*, 4(4), 1288-1292.
- Merchan-Merchan, W., Saveliev, A. V., & Taylor, A. M. (2008). High rate flame synthesis of highly crystalline iron oxide nanorods. *Nanotechnology*, 19(12), 125605.
- Zhang, S., Shan, J., Zhu, Y., Nguyen, L., Huang, W., Yoshida, H., ... & Tao, F. (2013). Restructuring transition metal oxide nanorods for 100% selectivity in reduction of nitric oxide with carbon monoxide. *Nano letters*, 13(7), 3310-3314.
- Wu, Y., Xiang, J., Yang, C., Lu, W., & Lieber, C. M. (2004). Single-crystal metallic nanowires and metal/semiconductor nanowire heterostructures. *Nature*, 430(6995), 61-65.
- Okada, K., Ricco, R., Tokudome, Y., Styles, M. J., Hill, A. J., Takahashi, M., & Falcaro, P. (2014). Copper conversion into Cu(OH)<sub>2</sub> nanotubes for positioning Cu<sub>3</sub>(BTC)<sub>2</sub> MOF crystals: controlling the growth on flat plates, 3D architectures, and as patterns. *Advanced functional materials*, 24(14), 1969-1977.
- Meyer, B., Padilla, J., & Vanderbilt, D. (1999). Theory of PbTiO<sub>3</sub>, BaTiO<sub>3</sub>, and SrTiO<sub>3</sub> surfaces. *Faraday Discussions*, 114, 395-405.
- Lebedev, A. I. (2009). Ab initio calculations of phonon spectra in A TiO<sub>3</sub> perovskite crystals (A= Ca, Sr, Ba, Ra, Cd, Zn, Mg, Ge, Sn, Pb). *Physics of the solid state*, 51(2), 362-372.
- Demirors, A. F., & Imhof, A. (2009). BaTiO<sub>3</sub>, SrTiO<sub>3</sub>, CaTiO<sub>3</sub>, and Ba<sub>x</sub>Sr<sub>1-x</sub>TiO<sub>3</sub> particles: A general approach for monodisperse colloidal perovskites. *Chemistry of materials*, 21(13), 3002-3007.
- Im, B., Jun, H., Lee, K. H., & Lee, J. S. (2011). Fabrication of nanoporous MTiO<sub>3</sub> (M= Pb, Ba, Sr) perovskite array films with unprecedented high structural regularity. *CrystEngComm*, 13(24), 7212-7215.
- Deng, H., Qiu, Y., & Yang, S. (2009). General surfactant-free synthesis of MTiO<sub>3</sub> (M= Ba, Sr, Pb) perovskite nanostrips. *Journal of Materials Chemistry*, 19(7), 976-982.
- Lin, Z. H., Yang, Y., Wu, J. M., Liu, Y., Zhang, F., & Wang, Z. L. (2012). BaTiO<sub>3</sub> nanotubes-based flexible and transparent nanogenerators. *The journal of physical chemistry letters*, 3(23), 3599-3604.
- Lin, M. F., Thakur, V. K., Tan, E. J., & Lee, P. S. (2011). Dopant induced hollow BaTiO<sub>3</sub> nanostructures for application in high performance capacitors. *Journal of Materials*

- Chemistry*, 21(41), 16500-16504.
13. Yasui, K., & Kato, K. (2012). Dipole–dipole interaction model for oriented attachment of BaTiO<sub>3</sub> nanocrystals: a route to mesocrystal formation. *The Journal of Physical Chemistry C*, 116(1), 319-324.
  14. Qin, S., Liu, D., Zuo, Z., Sang, Y., Zhang, X., Zheng, F., ... & Xu, X. G. (2010). UV-irradiation-enhanced ferromagnetism in BaTiO<sub>3</sub>. *The Journal of Physical Chemistry Letters*, 1(1), 238-241.
  15. Yang, J., Zhang, J., Liang, C., Wang, M., Zhao, P., Liu, M., ... & Che, R. (2013). Ultrathin BaTiO<sub>3</sub> nanowires with high aspect ratio: a simple one-step hydrothermal synthesis and their strong microwave absorption. *ACS applied materials & interfaces*, 5(15), 7146-7151.
  16. Da Silva, L. F., Avansi, W., Andrés, J., Ribeiro, C., Moreira, M. L., Longo, E., & Mastelaro, V. R. (2013). Long-range and short-range structures of cube-like shape SrTiO<sub>3</sub> powders: microwave-assisted hydrothermal synthesis and photocatalytic activity. *Physical Chemistry Chemical Physics*, 15(29), 12386-12393.
  17. Zheng, Z., Huang, B., Qin, X., Zhang, X., & Dai, Y. (2011). Facile synthesis of SrTiO<sub>3</sub> hollow microspheres built as assembly of nanocubes and their associated photocatalytic activity. *Journal of colloid and interface science*, 358(1), 68-72.
  18. Souza, A. E., Santos, G. T. A., Barra, B. C., Macedo Jr, W. D., Teixeira, S. R., Santos, C. M., ... & Longo, E. (2012). Photoluminescence of SrTiO<sub>3</sub>: influence of particle size and morphology. *Crystal growth & design*, 12(11), 5671-5679.
  19. Hu, Y., Tan, O. K., Pan, J. S., & Yao, X. (2004). A new form of nanosized SrTiO<sub>3</sub> material for near-human-body temperature oxygen sensing applications. *The Journal of Physical Chemistry B*, 108(30), 11214-11218.
  20. Wang, D., Liu, Y., Hu, H., Zeng, Z., Zhou, F., & Liu, W. (2008). Electrochemical characterization of the solution accessibility of CaTiO<sub>3</sub> microstructures and improved biomineralization. *The Journal of Physical Chemistry C*, 112(41), 16123-16129.
  21. Li, J., Zhang, Y. C., Wang, T. X., & Zhang, M. (2011). Low temperature synthesis and optical properties of CaTiO<sub>3</sub> nanoparticles from Ca (NO<sub>3</sub>)<sub>2</sub> · 4H<sub>2</sub>O and TiO<sub>2</sub> nanocrystals. *Materials Letters*, 65(11), 1556-1558.
  22. Ohtsu, N., Sato, K., Yanagawa, A., Saito, K., Imai, Y., Kohgo, T., ... & Hanawa, T. (2007). CaTiO<sub>3</sub> coating on titanium for biomaterial application—Optimum thickness and tissue response. *Journal of Biomedical Materials Research Part A: An Official Journal of The Society for Biomaterials, The Japanese Society for Biomaterials, and The Australian Society for Biomaterials and the Korean Society for Biomaterials*, 82(2), 304-315.
  23. Huang, C. L., & Weng, M. H. (2001). Improved high Q value of MgTiO<sub>3</sub>-CaTiO<sub>3</sub> microwave dielectric ceramics at low sintering temperature. *Materials Research Bulletin*, 36(15), 2741-2750.
  24. Phani, A. R., Passacantando, M., & Santucci, S. (2000). Synthesis and characterization of cadmium titanium oxide powders by sol-gel technique. *Journal of materials science*, 35(21), 5295-5299.
  25. Imran, Z., Batool, S. S., Jamil, H., Usman, M., Israr-Qadir, M., Shah, S. H., ... & Willander, M. (2013). Excellent humidity sensing properties of cadmium titanate nanofibers. *Ceramics International*, 39(1), 457-462.
  26. Z, Imran., M, A. Rafiq., M, Ahmad., K, Rasool., S, S. Batool., M, M. Hasan. (2013). AIP Adv.3, 032146-032159
  27. Karunakaran, C., & Vijayabalan, A. (2013). Electrical and optical properties of polyethylene glycol-assisted sol–gel solid state reaction-synthesized nanostructured CdTiO<sub>3</sub>. *Materials science in semiconductor processing*, 16(6), 1992-1996.
  28. Mohammadi, M. R., & Fray, D. J. (2009). Low-temperature perovskite-type cadmium titanate thin films derived from a simple particulate sol–gel process. *Acta materialia*, 57(4), 1049-1059.
  29. Hou, R. Z., Ferreira, P., & Vilarinho, P. M. (2011). Fabrication of BaTiO<sub>3</sub>–Carbon Nanocomposite and Porous BaTiO<sub>3</sub>. *Crystal growth & design*, 11(12), 5215-5220.
  30. Maxim, F., Ferreira, P., Vilarinho, P. M., & Reaney, I. (2008). Hydrothermal synthesis and crystal growth studies of BaTiO<sub>3</sub> using Ti nanotube precursors. *Crystal Growth and Design*, 8(9), 3309-3315.
  31. Bai, H., & Liu, X. (2013). Low temperature solvothermal synthesis, optical and electric properties of tetragonal phase BaTiO<sub>3</sub> nanocrystals using BaCO<sub>3</sub> powder. *Materials Letters*, 100, 1-3.
  32. Li, H. L., Du, Z. N., Wang, G. L., & Zhang, Y. C. (2010). Low temperature molten salt synthesis of SrTiO<sub>3</sub> submicron crystallites and nanocrystals in the eutectic NaCl–KCl. *Materials Letters*, 64(3), 431-434.
  33. Yang, S., Kou, H., Wang, H., Cheng, K., & Wang, J. (2010). Preparation and band energetics of transparent nanostructured SrTiO<sub>3</sub> film electrodes. *The Journal of Physical Chemistry C*, 114(2), 815-819.
  34. Huang, Y. J., Chiu, H. T., & Lee, C. Y. (2009). Growth of CaTiO<sub>3</sub> dendrites and rectangular prisms through a wet chemical method. *CrystEngComm*, 11(9), 1904-1909.
  35. Wang, D., Guo, Z., Chen, Y., Hao, J., & Liu, W. (2007). In situ hydrothermal synthesis of nanolamellate CaTiO<sub>3</sub> with controllable structures and wettability. *Inorganic chemistry*, 46(19), 7707-7709.
  36. Yang, L. Y., Feng, G. P., Wang, T. X., Zhang, J. M., & Lou, T. J. (2011). Low temperature preparation and characterization of CdTiO<sub>3</sub> nanoplates. *Materials Letters*, 65(17-18), 2601-2603.
  37. Yang, M., & DiSalvo, F. J. (2012). Template-free synthesis of mesoporous transition metal nitride materials from ternary cadmium transition metal oxides. *Chemistry of Materials*, 24(22), 4406-4409.
  38. Wang, Y., Xu, H., Wang, X., Zhang, X., Jia, H., Zhang, L., & Qiu, J. (2006). A general approach to porous crystalline TiO<sub>2</sub>, SrTiO<sub>3</sub>, and BaTiO<sub>3</sub> spheres. *The Journal of Physical Chemistry B*, 110(28), 13835-13840.
  39. Demirors, A. F., & Imhof, A. (2009). A general approach for monodisperse colloidal perovskites, Chemistry of

- 
- Materials. *Chemistry of Materials*, 21, 3002-3007.
40. Deng, H., Qiu, Y., & Yang, S. (2009). General surfactant-free synthesis of  $\text{MTiO}_3$  (M= Ba, Sr, Pb) perovskite nanostrips. *Journal of Materials Chemistry*, 19(7), 976-982.
  41. Dong, W., Li, B., Li, Y., Wang, X., An, L., Li, C., ... & Shi, Z. (2011). General approach to well-defined perovskite  $\text{MTiO}_3$  (M= Ba, Sr, Ca, and Mg) nanostructures. *The Journal of Physical Chemistry C*, 115(10), 3918-3925.
  42. Su, K., Nuraje, N., & Yang, N. L. (2007). Open-Bench Method for the Preparation of  $\text{BaTiO}_3$ ,  $\text{SrTiO}_3$ , and  $\text{Ba}_x\text{Sr}_{1-x}\text{TiO}_3$  Nanocrystals at  $80^\circ\text{C}$ . *Langmuir*, 23(23), 11369-11372.
  43. Qi, J., Li, L., Wang, Y., & Gui, Z. (2004). Preparation of nanoscaled  $\text{BaTiO}_3$  powders by DSS method near room temperature under normal pressure. *Journal of crystal growth*, 260(3-4), 551-556.
  44. Qi, J. Q., Wang, Y., Chen, W. P., Li, L. T., & Chan, H. L. W. (2005). Direct large-scale synthesis of perovskite barium strontium titanate nano-particles from solutions. *Journal of solid state chemistry*, 178(1), 279-284.
  45. Beier, C. W., Cuevas, M. A., & Brutchey, R. L. (2008). Room-Temperature Synthetic Pathways to Barium Titanate Nanocrystals. *Small*, 4(12), 2102-2106.
  46. Qi, J. Q., Peng, T., Hu, Y. M., Sun, L., Wang, Y., Chen, W. P., ... & Chan, H. L. W. (2011). Direct synthesis of ultrafine tetragonal  $\text{BaTiO}_3$  nanoparticles at room temperature. *Nanoscale research letters*, 6(1), 466.
  47. Yang, X., Fu, J., Jin, C., Chen, J., Liang, C., Wu, M., & Zhou, W. (2010). Formation mechanism of  $\text{CaTiO}_3$  hollow crystals with different microstructures. *Journal of the American chemical society*, 132(40), 14279-14287.
  48. Zhang, Q., Li, X., Ren, Z., Han, G., & Mao, C. (2015). Synthesis of  $\text{CaTiO}_3$  nanofibers with controllable drug-release kinetics. *European journal of inorganic chemistry*, 2015(27), 4532-4538.
  49. W, Dong., Q, Bao., X, Gu., G, Zhao., J, Cerac. (2015). *Soc. Jpn.* 123, 643-648.
  50. Fujinami, K., Katagiri, K., Kamiya, J., Hamanaka, T., & Koumoto, K. (2010). Sub-10 nm strontium titanate nanocubes highly dispersed in non-polar organic solvents. *Nanoscale*, 2(10), 2080-2083.
  51. Niederberger, M., Garnweitner, G., Pinna, N., & Antonietti, M. (2004). Nonaqueous and halide-free route to crystalline  $\text{BaTiO}_3$ ,  $\text{SrTiO}_3$ , and (Ba, Sr)  $\text{TiO}_3$  nanoparticles via a mechanism involving C-C bond formation. *Journal of the American Chemical Society*, 126(29), 9120-9126.
  52. Kumar, B., Saha, S., Ganguly, A., & Ganguli, A. K. (2014). A facile low temperature ( $350^\circ\text{C}$ ) synthesis of  $\text{Cu}_2\text{O}$  nanoparticles and their electrocatalytic and photocatalytic properties. *Rsc Advances*, 4(23), 12043-12049.

**Copyright:** ©2026 Bharat Kumar, et al. This is an open-access article distributed under the terms of the Creative Commons Attribution License, which permits unrestricted use, distribution, and reproduction in any medium, provided the original author and source are credited.